

Molecular and Histological Study of the Single and Combined Effects of Trastuzumab and Docetaxel on Fetal Rat Liver

Hays S. Mohammad Ameen, Ph.D* Janan H. Abdul-Fattah,**

ABSTRACT

Background: Trastuzumab (TZM) and docetaxel (DTX) are commonly employed in the treatment of breast cancer. This study aimed to investigate the histopathological and molecular effects of TZM and DTX alone and in combination on fetal rat liver.

Materials and Methods: Forty pregnant albino rats were divided into four equal groups. Group 1 was used as the control group and injected with normal saline only. Group 2 (TZM alone) was injected subcutaneously with TZM at a dose of 10 mg/kg body weight. Group 3 (DTX alone) was injected intraperitoneally with DTX at a dose of 15 mg/kg body weight. Group 4 (TZM and DTX combination) was injected with a combination of TZM (10 mg/kg) and DTX (15 mg/kg). All groups were injected on the 6th day of gestation. The pregnant rats from the control and treated groups were sacrificed on day 19 of gestation.

Results: As demonstrated in our study, the histological examination of fetal liver sections of the TZM alone (Group 2) and DTX alone (Group 3) revealed several histopathological alterations, while the TZM and DTX combination (Group 4) showed severe histopathological lesions of hepatic cords and their vasculatures. On the molecular level, the results of this study revealed many mutation types in exon 1 of the BCL2 gene, such as deletion, transition, and transversion after exposure to DTX alone and a combination of TZM and DTX, but the mutation level was higher in the combination treatment, while in exon 24 of the ErbB2/HER2 gene no mutation had occurred.

Conclusion: These findings confirmed the occurrence of a synergistic effect between TZM and DTX, which caused more severe damage to the liver of albino rat fetuses than the effect of either therapy alone and increased DNA mutation levels.

Keywords: Trastuzumab, docetaxel, fetal liver

INTRODUCTION

The period of pregnancy is considered one of the most important and critical periods in the lives of the mother and fetus. During pregnancy, the fetal liver undergoes significant functional and morphological changes, characterized by an increase in both the number and size of hepatocytes. The liver of the fetus is most vulnerable to detrimental exposure and is at the hazard of major liver diseases associated with birth^{1,2}.

TZM is a humanized recombinant monoclonal antibody that acts by blocking the human epidermal growth factor receptor 2 (HER2), which efficiently minimizes the mortality rate in patients with a variety of malignancies, including breast, colorectal, and gastric cancer³⁻⁵. Besides its usage combined with chemotherapy agents, TZM has demonstrated a good prognosis when combined with other anticancer drugs⁶.

The taxanes exemplify the backbone of numerous systemically antitumor treatment regimens for both early-stage and advanced-stage solid tumors⁷. DTX is a strong taxane that acts as an antitumor by intervening with a microtubule network that is essential to the mitosis of cells and interphase cellular function⁸. Currently, DTX has been broadly utilized as an intravenous anticancer medication for solid malignancies such as prostate, non-small cell lung, and breast cancer⁹.

In the latest years, a combination treatment of concurrent administration of many drugs has proved to be superior to using a single medication in clinical settings, consequently lowering the occurrence of multi-drug resistance¹⁰. A study done by Feng *et al.*¹¹ reported that TZM combined with DTX effectively improves the clinical effectiveness of patients with HER2-positive breast cancer and decreases levels of serum tumor markers and inflammatory factors. Another study showed a favorable clinical impact of TZM and DTX combination therapy in treating metastatic HER2-positive extramammary Paget's disease (EMPD)¹².

Considering the significance of the fetal liver, and it is the first organ exposed to chemotherapy, however, there are no studies available on the impacts of TZM and DTX, either alone or in combination, on the histopathology and molecular of the fetal liver. Therefore, this study aims to investigate the histopathological and molecular effects of TZM and DTX, both individually and in combination, on fetal albino rat livers.

MATERIALS AND METHODS

Ethical consideration

This study was approved by the Scientific Committee at the University of Duhok/College of Science/Department of Biology (reference number: 107 in June 6, 2021), as part of the fulfillment of the requirements for

* PhD Student, Department of Biology, College of Science, University of Duhok, Duhok, Iraq.

Email: hays.ameen@uod.ac

** Professor, Department of Biology, College of Science, University of Mosul, Mosul, Iraq.

Email: Janhsbio7@mosul.edu.iq

the corresponding author's Ph.D. degree.

Experimental animals

The present study was carried out on forty healthy adult virgin female Wistar albino rats (*Rattus norvegicus*) aged 12-14 weeks old, and their average weights ranged from 160 to 220 gm. The experiment was conducted in the animal house of the Biology Department, College of Science, Duhok University, Iraq. In accordance with ethics and accepted laboratory rules, the animals were housed in plastic cages and kept in controlled environmental conditions of temperature (25-30 °C), ventilation, and light cycle (12 hours light and 12 hours dark per day). During the experiment period, the animals were fed with standard pellets and water *ad libitum*.

The Mating procedure

The adult virgin female albino rats were mated overnight with fertile males at a ratio of 2 females and 1 male per cage. The following morning, the mating was confirmed by a vaginal smear taken from female rats and examined microscopically to check for sperm. The presence of spermatozoa in the vaginal smears was considered day zero of pregnancy.

Test anti-cancer drugs

Herceptin®, a brand name of the targeted cancer drug TZM, in the dosage form of 440 mg/20 mL, and Taxotere®, the commercial formulation of DTX, in the dosage form of 80 mg/10 mL, were obtained from the Oncology Department of the Azadi Teaching Hospital, Duhok, Iraq.

Experimental design

Forty pregnant albino rats were divided into four equal groups; each group has ten pregnant rats, which were injected on the sixth day of gestation, as follows:

Group 1 (Control): The pregnant rats were injected with normal saline only.

Group 2 (TZM Alone): The pregnant rats were injected subcutaneously with TZM at a dose of 10 mg/kg body weight.

Group 3 (DTX Alone): The pregnant rats were injected intraperitoneally with DTX at a dose of 15 mg/kg body weight.

Group 4 (TZM and DTX Combination): The pregnant rats were injected with a combination of TZM (10 mg/kg) and DTX (15 mg/kg).

Histopathological study

The fetuses were fixed in Bouin's fixative for 24 hours, followed by washing in 70% ethanol several times for picric acid removal, and then stored in 70% ethanol. After fixation, they were dehydrated through an ascending grade of alcohol, cleared by xylene, and embedded in the paraffin wax. Thereafter, the blocks of paraffin-embedded fetuses were cut to 5 µm of thickness, mounted on slides glass, and stained with hematoxylin and eosin (H&E). The slides were examined with a Motic light microscope to find out the histopathological alterations in the fetal liver.

Molecular study

DNA Extraction

Genomic DNA was extracted from 40 rat fetal liver tissue samples according to the protocol of Geneaid™ DNA Isolation Kit, a product that is commercially available and produced by Geneaid Biotech Ltd., Taiwan.

Estimation of concentration and purity of extracted DNA

The Nanodrop apparatus was used to estimate the extracted DNA concentration, while the DNA purity was assessed by calculating the absorbance 260/280 ratio.

Detection of ErbB2/HER2 and BCL2 genes by conventional PCR technique

The ErbB2/HER2 and BCL2 genes had been detected in the rat fetal liver tissue samples by conventional PCR technique as follows: four microliters (100 nanograms) of template DNA and one microliter (10 picompl) of each gene-specific primer were added to the contents of the master mix. The primer sequences for the ErbB2/HER2 and BCL2 genes are new design primers that include the coding regions of these two genes (Table 1). The primers were synthesized by Macrogen Company, South Korea.

Table 1. Primer sequences used in C-PCR.

PCR product size	Annealing Temp.	Primer Sequence (5' -3')	Gene
644 bp.	57 °C	F: TTCTGATTCTTCCC-GTCCTC	HER2
		R: TGGCAGAAGGTAT-GTCACGA	
613 bp.	57 °C	F: TAAAGGAAAACA-CACCTGATTTTA	BCL2
		R: GACCACAGGTGGCA-CAGG	

Afterwards, the reaction tubes were placed in the thermocycler apparatus to perform the multiplex reaction, utilizing the special reaction program (Table 2).

Table 2. The ErbB2/HER2 and BCL2 genes amplification program.

No. of Cycles	Time	Temperature (°C)	Stage	No.
1	5 min.	95	Initial denaturation	
	45 sec.	95	denaturation	
35	1 min.	57	Annealing	
	1 min.	72	Extension	
1	7 min.	72	Final extension	

The electrophoresis analysis of conventional PCR products

The amplified C-PCR products were analyzed for the ErbB2/HER2 and BCL2 genes on a 2% concentration of agarose gel. Electrophoresis was carried out at 5 V/cm for 1.5-2 hours, and the gel was viewed under an ultraviolet (UV) transilluminator and photographed by the gel documentary system.

DNA sequencing of genes

The C-PCR products of 40 DNA samples were sent to Psomagen USA to read the sequences and identify the variations of the ErbB2/HER2 and BCL2 genes based on the Sanger method. The sequences of nucleotides were aligned with DNA sequences available in the National Center for Biotechnology Information (NCBI) GenBank database by using the BLAST tool.

RESULTS

Histological and Histopathological Examination

Group 1: Histological Structure of the Liver of Albino Rat Fetuses

The light microscopic examination of the fetal liver sections in the

control group at the 19th day-old fetuses illustrated normal appearance, as demonstrated in the figure (1). This figure revealed that the liver at this stage of development displayed unclearly defined hepatic lobules and each lobule is composed of primitive hepatocytes tied up as disorganized, branched, and linked ribbons raying from a central vein towards the periphery. These cords of primitive hepatocytes are segregated by blood sinusoids.

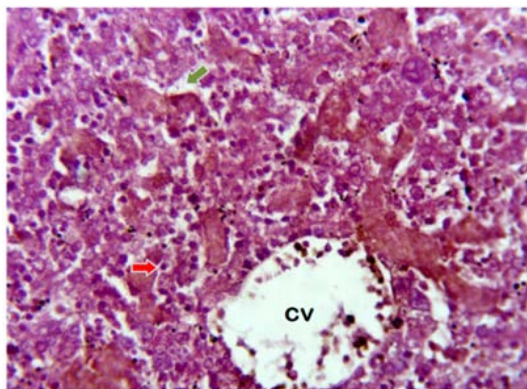


Figure 1. A photomicrograph of the transverse section of the fetal liver of 19-day-old albino rat fetuses of the control group showing: the normal histological structure of the liver tissue: central vein (CV), hepatocytes (red arrow), and blood sinusoid (green arrow) (H&E, 400x).

Group 2: Effect of TZM (10 mg/kg) on the Liver of Albino Rat Fetuses

The liver of the rat fetuses maternally injected with TZM alone exhibited many histopathological alterations. These alterations include sever congestion of sinusoids and blood capillaries, dilation of central vein, and hemorrhage in the hepatic tissue. The fetal hepatocytes possessed various abnormal cytological changes, including apoptosis and necrosis of primitive hepatocytes. Other hepatocytes displayed swelling and vacuolar degeneration in primitive hepatocytes (Figure 2).

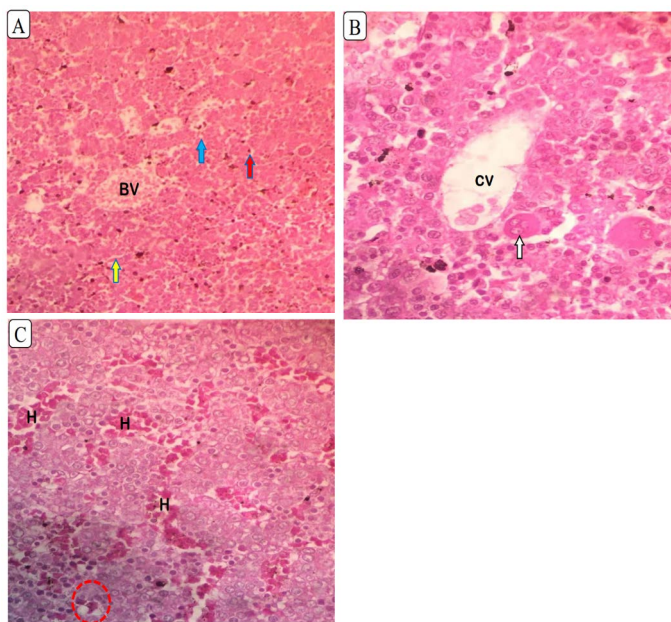


Figure 2. A photomicrograph of the transverse section through the fetal liver of 19-day old albino rat fetuses of the 10 mg/kg TZM alone treated group showing: (A) vacuolar degeneration (blue arrow) and necrosis (red arrow) of primitive hepatocytes, congested blood vessel (BV), and

sever congestion of sinusoids (yellow arrow). (B) dilated central vein (CV) with swelling of hepatocytes (white arrow). (C) hemorrhage (H), and apoptotic bodies (red circle) (H&E; A, B, and C 400x).

Group 3: Effect of DTX (15 mg/kg) on the Liver of Albino Rat Fetuses

The liver of 19-day-old albino rat fetuses maternally treated with DTX alone showed different hepatic histopathological changes including vacuolar degeneration of hepatocytes, coagulative necrosis of hepatocytes, and the formation of apoptotic bodies. Also, the fetal liver displayed an important abnormality in this treated group; the tissue demonstrated that this concentration caused the formation of hepatic steatosis which is classified into two types: macrovesicular and microvesicular steatoses. Besides, ballooning hepatocytes were observed, which are characterized as inflated hepatocytes with rarefied cytoplasm. Other effects of this treatment included dilation and congestion of the central vein and dilation of the sinusoids. In addition, the hemorrhage was seen inside the sinusoids (Figure 3).

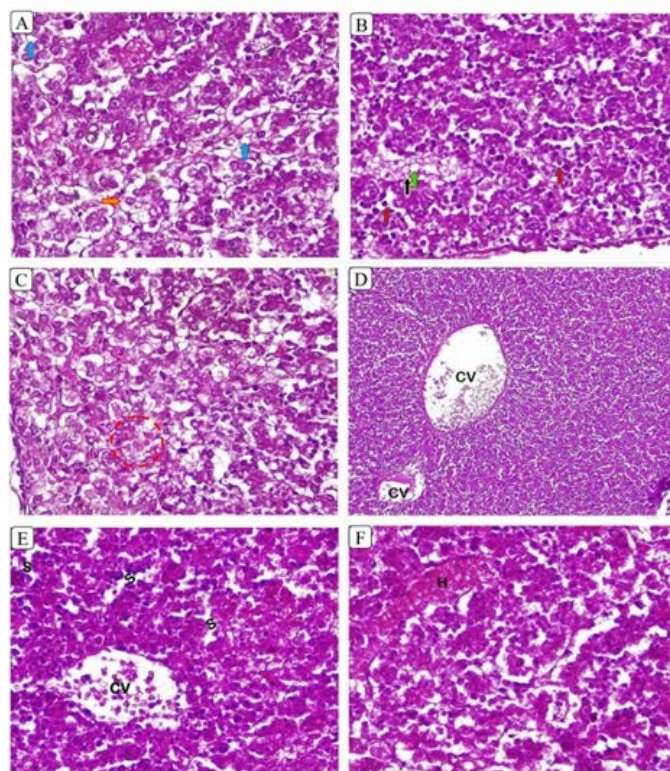


Figure 3. A photomicrograph of the transverse section of the fetal liver of 19-day-old albino rat fetuses of the 15 mg/kg DTX-treated group showing: (A) vacuolar degeneration (blue arrow), and ballooned primitive hepatocytes (orange arrow). (B) macrovesicular steatosis (green arrow), microvesicular steatosis (black arrow), and coagulative necrosis (red arrow) of hepatocytes. (C) the formation of apoptotic bodies (red circle). (D) dilated and congested of central vein (CV). (E) congested central vein (CV) and dilated blood sinusoids (S). (F) hemorrhage (H) was seen inside the sinusoids (H&E; A, B, C 400x, D 100x, E, and F 400x).

Group 4: Effect of a Combination of TZM (10 mg/kg) and DTX (15 mg/kg) on the Liver of Albino Rat Fetuses

The histological examination of the hepatic tissue of the rat fetuses maternally treated with a combination of TZM and DTX displayed severe histopathological lesions of hepatic cords and their vasculatures. These lesions include degeneration and necrosis of primitive hepatocytes, numerous of the primitive hepatocytes showed

pyknotic nuclei, and the formation of apoptotic bodies. Other impacts of this combination on the fetal hepatocytes were the formation of hepatic steatosis, which includes macrovesicular and microvesicular steatoses, and ballooning primitive hepatocytes. Besides, dilation and sever congestion of blood sinusoids, congestion of central veins, and vascular congestion associated with severe hemorrhage were detected in the fetal liver. The hemorrhage was seen inside the sinusoids, the central vein, and between the hepatocytes. Also, the combination of TZM and DTX caused hyperplasia of kupffer cells (Figure 4).

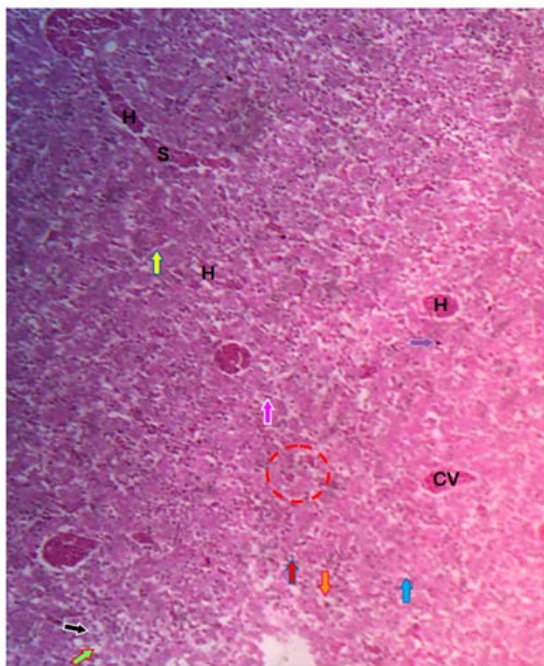


Figure 4. A photomicrograph of the transverse section of the fetal liver of 19-day old albino rat fetuses of the combination of TZM (10 mg/kg) and DTX (15 mg/kg) treated group showing: degeneration (blue arrow) and necrosis (red arrow) of primitive hepatocytes, pyknotic nuclei (purple arrow), apoptotic bodies (red circle), macrovesicular steatosis (green arrow), microvesicular steatosis (black arrow), ballooned primitive hepatocytes (orange arrow), dilated blood sinusoids (S), sever congested blood sinusoids (yellow arrow), congested central vein (CV), hemorrhage (H) was seen inside the sinusoids, the central vein, and between the hepatocytes and hyperplasia of kupffer cells (pink arrow) (H&E, 100x).

Molecular study of the ErbB2/HER2 and BCL2 genes

Genomic DNA Extraction

To study the genetic mutations in the ErbB2/HER2, and BCL2 genes and their relationship to congenital malformations, the genomic DNA was extracted from fetal liver tissue of the control and treated groups. The concentration of extracted DNA from treated and untreated samples was 30-50 ng/μl, and the extracted DNA purity of these samples was 1.8-1.9.

Amplification of the ErbB2/HER2 gene

The ErbB2/HER2 gene was amplified by a conventional polymerase chain reaction using specific designed primers (ErbB2/HER2/neu in rat forward primer: 5'-TTCTGATTCTTCCCGTCCTC-3' and ErbB2/HER2/neu in rat reverse primer: 5'-TGGCAGAAGGTATGTCACGA-3'). The outcomes displayed a single amplified product from both the control and treated groups, which has a molecular size of 644 bp (Figure 5).

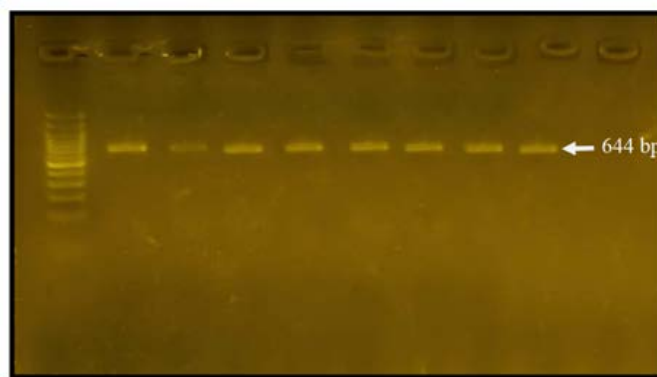
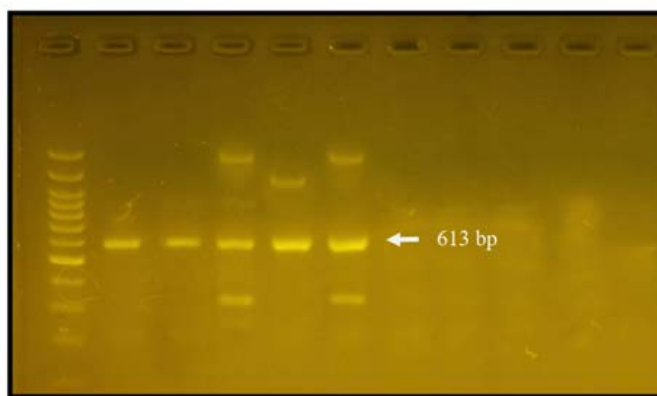


Figure 5. The amplification product of the ErbB2/HER2 gene, with a size of 644 bp. Conventional PCR amplified products on a 2% agarose gel.

Amplification of the BCL2 gene

The conventional PCR technique was employed to amplify the BCL2 gene by using specific designed primers (BCL2 forward primer: 5'-TAAAGGAAAACACACCTGATTTTA-3' and BCL2 reverse primer: 5'- GACCACAGGTGGCACAGG -3'). The results showed single DNA bands with a size of 613 bp in the untreated and treated groups (Figure 6).

Figure 6. The amplification product of the BCL2 gene, with a size of



613 bp. Conventional PCR amplified products on a 2% agarose gel.

Amplified product sequences of the ErbB2/HER2 and BCL2 genes

Comparison of ErbB2/HER2 and BCL2 gene sequences between control and NCBI theoretical sequences

The results of this study showed that there were no differences in ErbB2/HER2 and BCL2 gene sequences between the control and theoretical sequences from GenBank (NCBI) and the compatibility was 100%.

Comparison between fetuses ErbB2 gene sequences from the TZM alone group and theoretical sequences from NCBI

The results of the current study showed no differences between exon 24 of the fetuses ErbB2 gene sequences from the TZM alone group and NCBI sequences, with a compatibility of 100% (Figure 7).

Differences of BCL2 gene sequences in the fetuses of the DTX alone group compared with the NCBI theoretical sequences

In contrast, the anticancer drug DTX at a dose of 15 mg/kg revealed many mutation types in exon 1 of the BCL2 gene sequences, which include nine transition mutations, thirteen transversion mutations, and two deletion mutations compared with the theoretical sequences from GenBank (NCBI) as shown in figure (8) and Table (3).

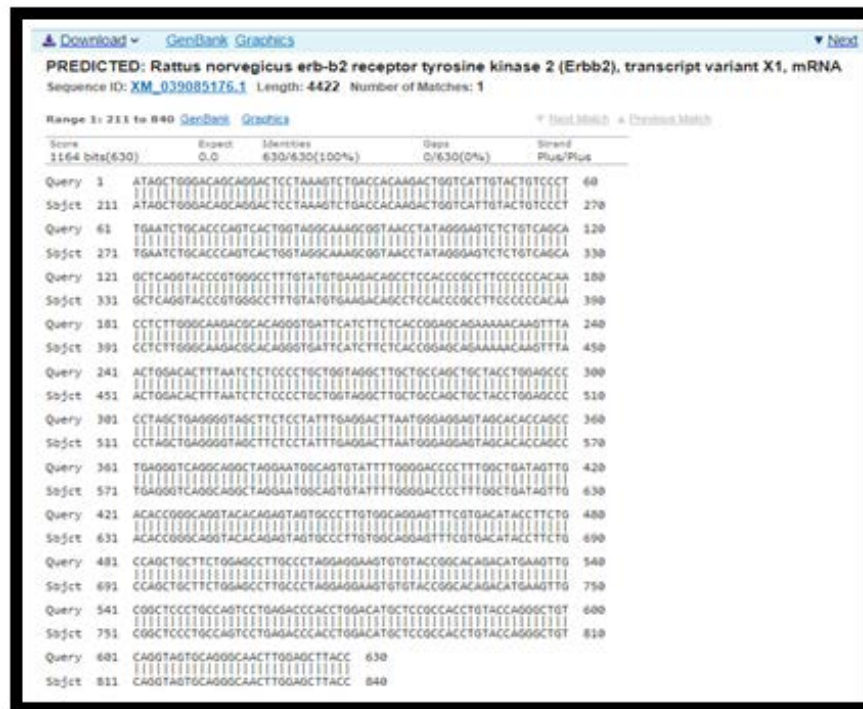


Figure 7. A comparison between the ErbB2/HER2 gene sequences of fetuses from the TZM alone group and NCBI theoretical sequences.

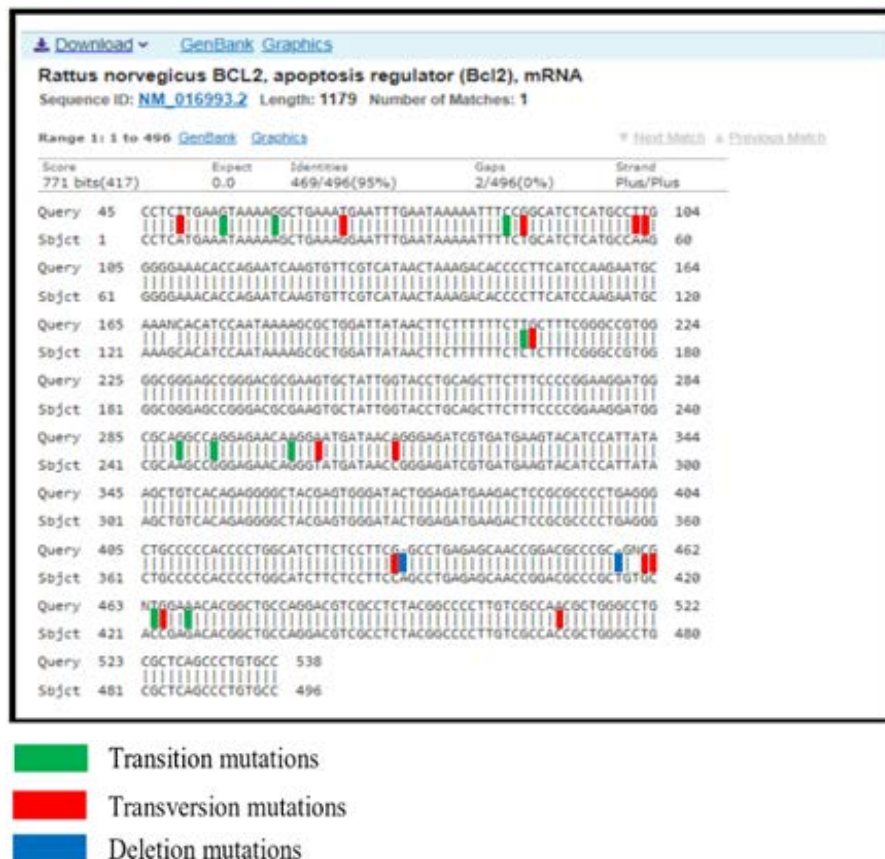


Figure 8. A comparison between the BCL2 gene sequences of fetuses from the DTX alone group and theoretical NCBI sequences. (The query number represents current data, while the subject represents the NCBI reference gene sequence).

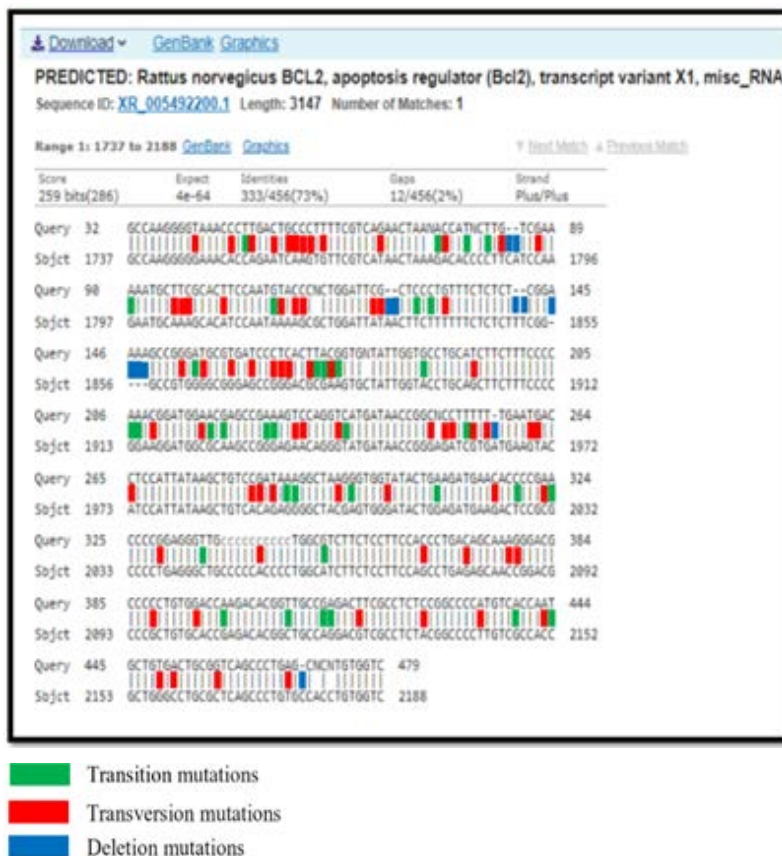


Figure 9. A comparison between the BCL2 gene sequences of fetuses from the combined group (TQM and DTX) and NCBI theoretical sequences.

Table 3. The various types of mutations that occurred in exon 1 of the BCL2 gene sequences of fetuses in the DTX alone group compared with the theoretical NCBI sequences.

Type of mutations	No. of mutations	Type of nucleotide sequence	Location in gene sequence
Transition mutations	9	G>A	10
		G>A	16
		C>T	43
		T>C	165
		G>A	245
		A>G	249
		A>G	258
		T>C	422
		A>G	426
Transversion mutations	13	T>A	5
		T>G	24
		G>T	45
		T>A	58
		T>A	59
		G>T	166
		A>T	261
		A>C	270
		G>C	390
		C>G	419
Deletion mutations	2	G>C	420
		G>C	423
		A>C	469
		->A	391
		->T	416

Table 4. The various types of mutations that occurred in exon 1 of the BCL2 gene sequences of fetuses in the combined group (TZA and DTX) compared with the theoretical NCBI sequences.

Type of mutations	No. of mutations	Type of nucleotide sequence	Location in gene sequence
Transition mutations	35	T>C	1753
		A>G	1780
		T>C	1784
		T>C	1787
		A>G	1797
		G>A	1817
		C>T	1837
		C>T	1839
		A>G	1865
		T>C	1882
		A>G	1883
		G>A	1885
		G>A	1897
		A>G	1913
		A>G	1914
		A>G	1924
		G>A	1926
		A>G	1932
		A>G	1933
		C>T	1943
		T>C	1960
		A>G	1995
		A>G	1996
		G>A	2004
		A>G	2016
		C>T	2027
		A>G	2032
		T>C	2043
		G>A	2060
		A>G	2106
		T>C	2115
		G>A	2120
		A>G	2121
		A>G	2147
		T>C	2152
Transversion mutations	69	T>G	1746
		C>A	1751
		T>A	1754
		C>A	1757
		G>C	1759
		C>A	1760
		C>A	1761
		C>G	1762
		T>G	1764
		G>T	1772
		C>A	1781
		G>T	1789
		G>C	1794
		T>A	1803
		T>A	1804
		C>A	1805
T>A	1810		
T>A	1818		
C>A	1820		

C>G	1821
C>A	1831
G>T	1832
G>T	1841
G>T	1863
T>G	1866
T>G	1870
T>G	1873
C>G	1876
T>G	1877
C>G	1878
T>G	1881
C>A	1884
T>G	1904
C>A	1916
A>C	1923
T>A	1936
C>A	1937
T>G	1942
C>G	1955
C>G	1957
C>A	1958
T>G	1961
T>G	1963
T>G	1969
G>T	1970
C>A	1973
C>A	1990
G>C	1991
T>G	1993
A>C	2002
T>G	2009
C>G	2024
A>C	2031
G>T	2037
C>A	2051
C>G	2074
C>G	2080
A>C	2086
G>C	2087
C>G	2096
G>C	2102
T>G	2125
C>A	2134
A>T	2142
A>C	2151
T>G	2157
A>C	2159
G>C	2165
A>T	2175
->C	1790
->A	1791
->A	1833
->A	1834
->T	1851
->T	1852
A>-	1855
A>-	1856
A>-	1857
A>-	1858
->A	1964
->C	2177

Deletion mutations

12

Differences between BCL2 gene sequences in the fetuses of the combined group (TZM and DTX) and NCBI theoretical sequences

Our study revealed many mutations in exon 1 of the BCL2 gene sequences in the combined group (TZM and DTX). These mutations were of many types, which include thirty-five transition mutations, sixty-nine transversion mutations and twelve deletion mutations, compared with the theoretical sequences from the NCBI GenBank, as shown in Figure (9) and Table (4).

DISCUSSION

The liver is an organ of vital importance responsible for the detoxifying and eliminating of toxic products. The medications in the mother's circulation first need to be transferred through placental barriers in order to enter the blood of the fetus, then travel across umbilical veins. A small amount of the blood will pass through the fetal liver prior to arriving at the heart, so the liver of the fetus is the first organ receiving placentally transmitted medication¹³.

The present study used TZM, which targets HER2, for gastric and breast cancer^{14,15}. Notably, there aren't any published studies on the histopathological effects of TZM on the fetal rat liver. To our comprehension, this is the first study of histological alterations in the liver of albino rat fetuses induced by this anti-HER2 (Neu/ErbB2) monoclonal antibody.

The current histological investigation demonstrated several histopathological alterations in the liver tissues of albino rat fetuses maternally treated with TZM alone such as sever congestion of sinusoids and blood capillaries in the hepatic tissue, and dilatation of central vein. According to Kumar *et al.*¹⁶, this could be due to an inflammatory reaction aroused by chemical mediators such as prostaglandin and histamine released by mast cells and other inflammatory cells that cause vasodilatation and a localized increase in blood flow that's associated with capillary bed engorgement, which becomes more permeable to protein-rich fluid, thereby raising the viscosity of blood and RBCs aggregate creating blood clots. These pathological events are mirrored microscopically as many dilation blood vessels filled by RBCs with congestion and clotting.

During the development of the embryo, vascular endothelial growth factor (VEGF) plays an important role in the embryonic vasculogenesis and angiogenesis¹⁷. The higher expression of HER2 (Neu/ErbB2) in the fetal rat liver is correlated with increased expression of VEGF. In the current study, the possible mechanism by which TZM-induced hemorrhage occurs in the liver of rat fetuses is by blocking ErbB2, which causes vascular disruption through inhibition of VEGF and leads to hemorrhage.

The hepatocytes of rat fetuses maternally treated with TZM alone showed the vacuolar degeneration of primitive hepatocytes. According to Torbenson and Washington¹⁸, vacuolar degeneration, which appeared as a foamy manifestation of the cytoplasm of the hepatocytes, was the outcome of an endoplasmic reticulum edema associated with a rise in the intracellular water.

The observed necrosis of the primitive hepatocytes in this study might be due to TZM causing the opening of the mitochondrial permeability transition pore (MPTP), an increased production of reactive oxygen species (ROS), and a depletion of ATP¹⁹. These alterations lead to a severe swelling of the mitochondrial permeability, which eventually results in necrotic fetal hepatocytes.

Among the significant findings of the present study was the observation of apoptotic hepatocytes. This result might be due to the blocking of

HER2 signaling by TZM downregulated Bcl-xL and upregulated Bcl-xS, which enhanced the mitochondrial intrinsic apoptotic pathway¹⁹. The same study also revealed that the binding of chemotherapeutic medications such as TZM to mitochondrial DNA (mtDNA) results in the stimulation of apoptosis by ROS generation and loss of the function of mitochondria.

DTX is a microtubule-active drug and one of the strongest cancer chemotherapeutics. It has piqued keen attention among numerous scientists worldwide due to its clinical usefulness in several solid tumors, such as breast, lung, stomach, head and neck, ovarian, and prostate cancers²⁰. However, because of DTX's poor solubility in water, the process of preparation needs to use a large number of Tween 80 (polysorbate 80) and a certain anhydrous ethanol to completely dissolve DTX^{21,22}.

However, there aren't any published studies on the histopathological effects of DTX on the fetal rat liver. To our comprehension, this is the first study of histological changes in the liver of albino rat fetuses induced by this antimicrotubule agent.

The hepatocytes of fetuses maternally treated with DTX alone showed apoptosis, and this might be attributed to the following two reasons. Firstly, DTX has the capacity to promote tubulin monomer polymerization and inhibit microtubule depolymerization, which are recognized to play main roles in intracellular trafficking, signaling, cell division, and migration. This disrupting of the normal balance of the tubulin function results in mitotic arrest at the G2/M phase of the cell cycle. Secondly, DTX can also induce apoptosis by stimulating BCL2 phosphorylation. It is well known that BCL2 prevents cells from apoptosis by dimerizing with the proapoptotic protein Bax. The phosphorylation of BCL2 caused by DTX results in the loss of its antiapoptotic function. Thus, DTX forces caspase cascade activation, which leads to increased apoptosis²³.

According to the current study, DTX was displayed to cause necrosis in fetal hepatic cells. There are two main reasons for this finding: either, this could be because of the strong cytotoxic impact of DTX, or this might be due to the excess amount of polysorbate 80 in its intravenous formulation²⁴.

The current study has shown the alteration of DTX in the lipid metabolism that was confirmed by the fatty degeneration noticed in the fetal liver tissue examination. This could be due to in-utero exposure to the ethanol contained in DTX. A study done by González-Flores and coworkers²⁵ reported that alcohol traverses the placenta through passive diffusion and quickly arrives at the fetus because of its low molecular weight and lipid solubility. The liver is the major site for the metabolism of alcohol; consequently, it is more susceptible to an injury related to alcohol²⁶. Many researchers attempted to explain the mechanisms of the accumulation of lipids in the hepatocytes induced by alcohol. Yang *et al.*²⁷ and Jeon and Carr²⁸ reported that the liver mostly favors alcohol as a source of energy, and due to this, it ceases utilizing fats, which accumulate in hepatocytes, resulting in a fatty liver. On the other hand, Yang *et al.*²⁷ reported that the hydrogen generated as a by-product of alcohol metabolism is transformed into more fat for the synthesis of lipoproteins and cholesterol, which further accumulate as droplets of fat in the liver.

The present study observed ballooned hepatocytes, which is considered a unique form of injury to hepatocytes, in the liver of rat fetuses maternally treated with DTX. Li and colleagues²⁹ stated in their study that these cells are round, large, and typically have a diameter around 1.5-2 times greater than that of normal hepatocytes. They are often

observed nearby steatotic hepatocytes or regions having perisinusoidal fibrosis. The markedly ballooned hepatocytes of maternally treated fetuses exhibited in the current investigation could be attributed to the disruption of microtubules and severe injury to cells induced by DTX.

Moreover, DTX treatment during the organogenesis of rats caused damage to the hepatic vasculatures of 19-day old albino rat fetuses, including dilated and congested appearance of the central vein and dilated of the hepatic sinusoids. This might be due to the inflammatory reaction that causes vasodilatation and a rise in vascular permeability, which results in fluid loss from the blood and the vessels appearing engorged with RBCs¹⁶. Hemorrhage was also observed in the fetal liver. A possible explanation for this outcome is that DTX causes potent functional damage to endothelial cells and leads to hemorrhage.

DTX is metabolized in the liver through the cytochrome P450 3A4 (CYP3A4)³⁰, and this is the fundamental method for the clearance of DTX. Patients with a low activity of CYP3A4 are at risk of decreased clearance, leading to increased DTX toxicity³¹. Robinson and colleagues³² revealed that the expression and activity of CYP3A4 are lower in the fetus than in the adult. Due to the low activity of this enzyme, DTX accumulates in the fetal liver, which subsequently leads to severe histopathological lesions of the hepatic cords and their vasculatures owing to its toxic effects.

In the present study, combined treatment of TZM and DTX exhibited severe histopathological changes in the fetal liver tissue, which manifested as degeneration, necrosis, apoptosis, and ballooning of primitive hepatocytes, as well as hepatic steatosis and hyperplasia of kupffer cells. Besides, dilated and sever congested of hepatic sinusoids, congested of central veins, and vascular congested associated with severe hemorrhage were detected. These findings confirmed the occurrence of a synergistic effect between TZM and DTX, which caused more severe damage to the liver of albino rat fetuses than the effect of either therapy alone. To our comprehension, this is the first study describing the histopathological effects of TZM and DTX on the liver of 19-day-old fetuses.

The results of the current study revealed that there were no differences in exon 24 of the ErbB2/HER2 gene sequences between the TZM alone group and control group, and this disclosed that this anticancer drug didn't affect this exon of gene sequences but might affect other exon or intron sequences.

As an important biological process, apoptosis is essential for the elimination of aged, undesirable, or seriously damaged cells throughout development as well as for maintaining cellular homeostasis in mature multicellular organisms^{33,34}. Many researchers pointed to cells undergo apoptosis via the two major pathways: intrinsic (mediated by mitochondria) and extrinsic (mediated by death receptors)^{35,36}, and is stimulated through a plenty of factors, including genotoxic and cellular stress³⁵.

The present study was selected the BCL2 (B-cell leukemia/lymphoma 2) gene, is the founding member of the Bcl-2 family of regulator proteins which inhibit or induce apoptosis. Among the BCL-2 protein family, BCL-2 is the most distinctive antiapoptotic protein. The protein is located on chromosome 18 and has a size of 26 ku. By forming a heterodimer with BAX, it can prevent apoptosis and maintain cell survival³⁷.

This study indicated a very variation in exon 1 of the BCL2 gene sequences; these variation mutations between treatment with DTX at a dose of 15 mg/kg and control include many point mutation such

as transition and transversion mutations beside the deletion mutation. Deletion and point mutations in the BCL2 gene have been shown to repeal the ability of BCL2 to heterodimerize with Bax and also rescind its function as a cell death inhibitor. According to Singh *et al.*³³ and Urbani *et al.*³⁸, this led to the formation of pores in the outer mitochondrial membrane resulting in a process known as MOMP (Mitochondrial Outer Membrane Permeabilization), which permits cytochrome C to spill into the cytoplasm, where it binds to APAF-1 (apoptotic protease activating factor 1), promoting its oligomerization, and binding to procaspase 9 to form a complex known as the apoptosome. At the apoptosome, procaspase 9 is activated through dimerization, which in turn cleaves and activates the executioner caspases-3 and -7, leading to increased apoptotic cell death.

Furthermore, the present study results indicated that when the pregnant female rats were treated with DTX alone during the gestation period mentioned previously, this treatment caused increased apoptosis in embryonic rat tissues via the intrinsic pathway. This excessive apoptosis caused adverse effects on the organogenesis and growth of fetal rats, and the severity of these effects was associated with the formation of congenital malformations in rat fetuses.

The results of the present study are in agreement with those obtained by Yoshida *et al.*³⁹ who showed that when mice were intraperitoneally exposed to DTX (5 mg/kg and 10 mg/kg), administration promoted the mitochondrial apoptotic pathway in granulosa cells, consequently enhancing the cleaved caspase-3 expression, a marker for apoptosis. The results obtained by Singh *et al.*⁴⁰ are also in agreement with the present result mentioned above. They showed that DTX-induced apoptosis in different cancer cells by regulation of Bcl-xL/Bcl-2 expression.

Although TZM's effectiveness is dependent on its interaction with HER2 (Neu/ErbB2) receptors, Abo-Zeid and colleagues⁴¹ found in their study on breast cancer cell lines that its impact arrived at the cytogenetic levels and induced widespread genotoxicity. They showed that TZM caused cell death by apoptosis, as well as micro-nuclei in bi-nucleated cells of MDA-MB-231 and MCF-7 cells. This observed damage to DNA was directly associated with the TZM concentration. They also found that TZM increased the expression of caspase-3 extensively through raising its concentration in these two kinds of cells. Other researchers found that TZM is renowned for inducing accelerated apoptosis of cardiomyocytes, which is distinguished by the downregulation of the expression of BCL2 and upregulation of the expressions of caspase-9 and caspase-3 in myocardial tissue^{42,43}.

The results of the current study revealed that TZM in combination with DTX elicits a synergistic effect on the BCL2 gene sequences. Our data revealed that the combination of TZM with DTX resulted in a high number of substitution or point mutations, which include transition mutations and transversion mutations as well as deletion mutations in exon 1 of the BCL2 gene sequences compared with DTX monotherapy. These high numbers of BCL2 mutations led to the abolishment of the ability of BCL2 to heterodimerize with Bax and also repealed its function as a cell death suppressor. According to Singh *et al.*³³ and Urbani *et al.*³⁸, this resulted in mitochondrial permeability transition pore (MPTP) opening, cytochrome c release, and a greater increase in caspase-9 and caspase-3 activities in embryonic rat tissues as compared with DTX treatment alone.

Therefore, the results of the current study demonstrated that the combination treatment of TZM and DTX on the 6th day of gestation increased DNA mutation levels that strongly induced apoptosis. This potent apoptotic impact caused severe adverse effects on the

organogenesis and growth of fetal rats, and the severity of these effects was associated with the formation of congenital abnormalities in rat fetuses. These molecular results confirmed the histopathological findings.

CONCLUSION

Our results demonstrated that combined treatment of TZM and DTX caused more severe damage to the liver tissue of albino rat fetuses than the effect of either therapy alone. On the molecular level, our study revealed many mutation types in exon 1 of the BCL2 gene, which were at a higher level in the combination therapy than in DTX alone. These results confirmed the occurrence of a synergistic effect between TZM and DTX in rat fetuses.

Authorship Contribution: All authors share equal effort contribution towards (1) substantial contributions to conception and design, acquisition, analysis and interpretation of data; (2) drafting the article and revising it critically for important intellectual content; and (3) final approval of the manuscript version to be published. Yes.

Potential Conflict of Interest: None

Competing Interest: None

Acceptance Date: 06-02-2025

REFERENCES

- García-Romero CS, Guzman C, Cervantes A, et al. Liver Disease in Pregnancy: Medical Aspects and Their Implications for Mother and Child. *Ann Hepatol* 2019; 18(4): 553-62.
- Gad El-Hak HN, Abdelrazek HM, Zeidan DW, et al. Assessment of Changes in the Liver of Pregnant Female Rats and Their Fetuses Following Monosodium Glutamate Administration. *Environ Sci Pollut Res Int* 2021; 28(32): 44432-41.
- Vega Cano KS, Marmolejo Castaneda DH, Escrivá-de-Romani S, et al. Systemic Therapy for HER2-Positive Metastatic Breast Cancer: Current and Future Trends. *Cancers (Basel)* 2022; 15(1): 51.
- Alsina M, Arrazubi V, Diez M, et al. Current Developments in Gastric Cancer: From Molecular Profiling to Treatment Strategy. *Nat Rev Gastroenterol Hepatol* 2023; 20(3): 155-70.
- Bando H, Ohtsu A, Yoshino T. Therapeutic Landscape and Future Direction of Metastatic Colorectal Cancer. *Nat Rev Gastroenterol Hepatol* 2023; 20(5): 306-22.
- Lin M, Xiong W, Wang S, et al. The Research Progress of Trastuzumab-Induced Cardiotoxicity in HER-2-Positive Breast Cancer Treatment. *Front Cardiovasc Med* 2022; 8: 821663.
- Muth M, Ojara FW, Kloft C, et al. Role of TDM-Based Dose Adjustments for Taxane Anticancer Drugs. *Br J Clin Pharmacol* 2021; 87(2): 306-16.
- Hertz D. Exploring Pharmacogenetics of Paclitaxel- and Docetaxel-Induced Peripheral Neuropathy by Evaluating the Direct Pharmacogenetic-Pharmacokinetic and Pharmacokinetic-Neuropathy Relationships. *Expert Opin Drug Metab Toxicol* 2021; 17(2): 227-39.
- Hendriks J, Stuurman F, Song J. No Relation between Docetaxel Administration Route and High-Grade Diarrhea Incidence. *Pharmacol Res Perspect* 2020; 8(4): e00633.
- Berrios-Caro E, Gifford DR, Galla T. Competition Delays Multidrug Resistance Evolution During Combination Therapy. *J Theor Biol* 2021; 509: 110524.
- Feng QZ, Chen XZ, Sun J, et al. Analysis of the Effect of Trastuzumab Combined with Docetaxel on Serum Tumor Markers in the Treatment of HER-2 Positive Breast Cancer and Factors Influencing Therapeutic Efficacy. *Cancer Manag Res* 2021; 13: 8077-84.
- Hirai I, Tanese K, Nakamura Y, et al. Phase II Clinical Trial of Docetaxel and Trastuzumab for HER2-Positive Advanced Extramammary Paget's Disease (EMPD-HER2DOC). *Oncologist* 2024; 29(9): e1201-e1208.
- Li D, Zhu Y, Donnelley M, et al. Fetal Drug Exposure After Maternally Administered CFTR Modulators Elexacaftor/Tezacaftor/Ivacaftor in a Rat Model. *Biomed Pharmacother* 2024; 171: 116155.
- Gradishar WJ, Anderson BO, Abraham J. Breast Cancer, NCCN Clinical Practice Guidelines in Oncology. *J Natl Compr Canc Netw* 2020; 18(4): 452-78.
- Ajani JA, D'Amico TA, Brentn DJ. Gastric Cancer, NCCN Clinical Practice Guidelines in Oncology. *J Natl Compr Canc Netw* 2022; 20(2): 167-92.
- Kumar V, Cotran R, Robbins L. Basic Pathology. 11th ed. USA: Churchill Livingstone, 2022.
- Pérez-Gutiérrez L, Ferrara N. Biology and Therapeutic Targeting of Vascular Endothelial Growth Factor A. *Nat Rev Mol Cell Biol* 2023; 24(11): 816-34.
- Torbenson M, Washington K: Pathology of Liver Disease. Advances in the Last 50 Years. *Hum Pathol* 2020; 95: 78-98.
- Gorini S, De Angelis A, Berrino L, et al. Chemotherapeutic Drugs and Mitochondrial Dysfunction: Focus on Doxorubicin, Trastuzumab, and Sunitinib. *Oxid Med Cell Longev* 2018; 2018: 7582730.
- Razak SA, Gazzali AM, Fisol FA. Advances in Nanocarriers for Effective Delivery of Docetaxel in the Treatment of Lung Cancer: An Overview. *Cancers (Basel)* 2021; 13(3): 400.
- Dawoud M, Abourehab MA, Abdou R. Monoolein Cubic Nanoparticles as Novel Carriers for Docetaxel. *J Drug Deliv Sci Technol* 2020; 56: 1-36.
- Gong F, Wang R, Zhu Z, et al. Drug-Interactive mPEG-b-Plaque(Boc) Micelles Enhance the Tolerance and Anti-tumor Efficacy of Docetaxel. *Drug Deliv* 2020; 27(1): 238-47.
- Imran M, Saleem S, Chaudhuri A, et al. Docetaxel: An Update on its Molecular Mechanisms, Therapeutic Trajectory and Nanotechnology in the Treatment of Breast, Lung and Prostate Cancer. *J Drug Deliv Sci Technol* 2020; 60: 1-18.
- Jha SK, Chung JY, Pangeni R, et al. Enhanced Antitumor Efficacy of Bile Acid-Lipid Complex-Anchored Docetaxel Nanoemulsion via Oral Metronomic Scheduling. *J Control Release* 2020; 328: 368-94.
- González-Flores D, Márquez A, Casimiro I. Oxidative Effects in Early Stages of Embryo Development Due to Alcohol Consumption. *Int J Mol Sci* 2024; 25(7): 4100.
- Hyun J, Han J, Lee C, et al. Pathophysiological Aspects of Alcohol Metabolism in the Liver. *Int J Mol Sci* 2021; 22(11): 5717.
- Yang L, Yang C, Thomes PG, et al. Lipophagy and Alcohol-Induced Fatty Liver. *Front Pharmacol* 2019; 10(5): 1-13.
- Jeon S, Carr R. Alcohol Effects on Hepatic Lipid Metabolism. *J Lipid Res* 2020; 61(4): 470-79.
- Li YY, Zheng TL, Xiao SY, et al. Hepatocytic Ballooning in Non-Alcoholic Steatohepatitis: Dilemmas and Future Directions. *Liver Int* 2023; 43(6): 1170-82.
- Lek RM, Ten Berg-Lammers LA, Van Nuland M. Docetaxel for Castrate-Resistant Prostate Cancer: The Effect of Hepatic Impairment at the Start of Therapy on the Incidence of Adverse Events. Msc. Thesis, Utrecht University Netherlands; 2024.

31. Powell NR, Shugg T, Ly RC, et al. Life-Threatening Docetaxel Toxicity in a Patient with Reduced-Function CYP3A Variants: A Case Report. *Front Oncol* 2022; 11: 809527.
32. Robinson JF, Hamilton EG, Lam J, et al. Differences in Cytochrome P450 Enzyme Expression and Activity in Fetal and Adult Tissues. *Placenta* 2020; 100: 35-44.
33. Singh R, Letai A, Sarosiek K. Regulation of Apoptosis in Health and Disease: The Balancing Act of BCL-2 Family Proteins. *Nat Rev Mol Cell Biol* 2019; 20(3): 175-93.
34. Qian S, Wei Z, Yang W, et al. The Role of BCL-2 Family Proteins in Regulating Apoptosis and Cancer Therapy. *Front Oncol* 2022; 12: 985363.
35. Westaby D, Jimenez-Vacas JM, Padilha A, et al. Targeting the Intrinsic Apoptosis Pathway: A Window of Opportunity for Prostate Cancer. *Cancers (Basel)* 2022; 14(1): 51.
36. Mohammadhosseinpour S, Weaver A, Sudhakaran M, et al. Arachidin-1, a Prenylated Stilbenoid from Peanut, Enhances the Anticancer Effects of Paclitaxel in Triple-Negative Breast Cancer Cells. *Cancers (Basel)* 2023; 15(2): 399.
37. Park HA, Broman K, Jonas EA. Oxidative Stress Battles Neuronal Bcl-xL in a Fight to the Death. *Neural Regen Res* 2021; 16(1): 12-5.
38. Urbani A, Prosdocimi E, Carrer A, et al. Mitochondrial Ion Channels of the Inner Membrane and Their Regulation in Cell Death Signaling. *Front Cell Dev Biol* 2021; 8: 620081.
39. Yoshida K, Erdenebayar O, Kadota Y, et al. Effect of Intraperitoneal Docetaxel on Ovarian Function in Mice. *J Obstet Gynaecol* 2022; 42(8): 3672-78.
40. Singh SK, Apata T, Gordetsky J, et al. Docetaxel Combined with Thymoquinone Induces Apoptosis in Prostate Cancer Cells via Inhibition of the PI3K/AKT Signaling Pathway. *Cancers (Basel)* 2019; 11(9): 1390.
41. Abo-Zeid MAM, Abo-Elfadl MT, Gamal-Eldeen Amira M. Trastuzumab Augments Apoptotic Cell Death of MCF-7 and MDA-MB-231 Breast Cancer Cell Lines. *J Pharm Sci Res* 2019; 11(2): 324-30.
42. Bulut G, Atmaca H, Karaca B. Trastuzumab in Combination with AT-101 Induces Cytotoxicity and Apoptosis in HER2 Positive Breast Cancer Cells. *Future Oncol* 2020; 16(3): 4485-95.
43. Méndez-Valdés G, Gómez-Hevia F, Bragato MC, et al. Antioxidant Protection Against Trastuzumab Cardiotoxicity in Breast Cancer Therapy. *Antioxidants (Basel)* 2023; 12(2): 457.